

Influence of Backing and Matching Layers in Ultrasound Transducers Performance

Valéria M. do Nascimento^{*a}, Vera Lúcia da S. Nantes Button^a, Joaquim M. Maia^b, Eduardo T. Costa^a and Eduardo J. V. Oliveira^a

^aUltrasound Laboratory, Dept. of Biomedical Engineering (DEB), Faculty of Electrical and Computing Engineering (FEEC) and Center of Biomedical Engineering (CEB) of the State University of Campinas (UNICAMP), SP, Brazil

^bFederal Center of Technology (CEFET), Curitiba, PR, Brazil

ABSTRACT

In this work we have investigated the influence of the backing layer composition and the matching layer thickness in the performance of ultrasound transducers constructed with piezoelectric ceramic discs. We have constructed transducers with backing layers of different compositions, using mixtures of epoxy with alumina powder and/or Tungsten powder and with $\lambda/4$ or $3\lambda/4$ thickness epoxy matching layers. The evaluation tests were performed in pulse-echo mode, with a flat target, and in transmission/reception mode, with a calibrated PVDF hydrophone. The acoustical field emitted by each transducer was mapped in order to measure the on-axis and transverse field profiles, the aperture size and the beam spreading. The bandwidths of the transducers were determined in pulse-echo mode. Comparing the evaluation tests results of two transducers constructed with the same backing layer, the one constructed with $\lambda/4$ thickness epoxy matching layer showed better performance. The results showed that the transducers constructed with epoxy, alumina and Tungsten powders backing layers have larger bandwidth. The larger depth of field was measured for transducers constructed with epoxy and Tungsten powder backing layers. These transducers and those constructed with epoxy, Tungsten and alumina powders backing layers showed the larger field intensities in the measured transverse profiles.

Keywords: Ultrasound Transducer, Piezoelectric Ceramic, Backing Layer, Matching Layer, Acoustical field

1. INTRODUCTION

Ultrasound transducer transforms electrical energy into mechanical energy and vice-versa, through its single or multiple piezoelectric elements. Ultrasound transducers can be constructed in several configurations according to their applications: non-destructive testing, tissue characterization, medical images, etc.

Many factors, including the type of piezoelectric element, the mechanical construction, the electrical matching and the mechanical and electrical loads, influence the performance of the transducer. The mechanical construction influences important parameters as the aperture size, the bandwidth and mechanical losses of the transducer [2] [6] [7] [8] [9].

In this work we have studied the influence of electrical matching, the thickness of the acoustical matching and the utilization of different materials to construct the backing layer, in the performance of a single element (piezoelectric ceramic disc) ultrasound transducer. We have tested the constructed transducers according to international standards [1] [3] [4] [5] measuring the electromechanical coupling factor of the thickness mode, bandwidth, aperture size, beam spread and transverse and on-axis profiles.

2. METHODOLOGY

This work was developed in two phases: the first one corresponded to the construction of the ultrasound transducers and the second one, the characterization of these transducers.

2.1. Construction of the ultrasound transducers

The steps of the transducers construction are: to determinate of the resonance and anti-resonance frequencies and the coupling factor of ceramic vibration modes (radial and thickness), to set up the electrical contact with ceramic electrodes, to place the backing and matching layers, to set up the electrical matching, to put an external covering and the cable that connects the transducer to a pulser/receiver.

Before the construction of the transducers, the impedance module and phase versus frequency curves of the ceramic discs were traced using an impedance analyzer. These curves allowed identifying the resonance frequency (f_r), at which the impedance module value is minimum, and the anti-resonance frequency (f_{ar}), at which the value is maximum. The effective coupling factor (k_{ef}) of each ceramic radial and thickness vibration modes were calculated according to Equation 1.

$$k_{ef}^2 = \frac{f_{ar}^2 - f_r^2}{f_{ar}^2} \quad (1)$$

The impedance module and phase versus frequency curves were also traced after each one of the construction steps, to verify any change in the radial and thickness frequencies and coupling factors.

The schematic diagram showed in Figure 1 presents the components of the ultrasound transducers constructed in this work. The active element used in the construction of these transducers was PZT-5A piezoelectric ceramic discs, 12mm diameter, 1mm thickness and 2MHz central frequency.

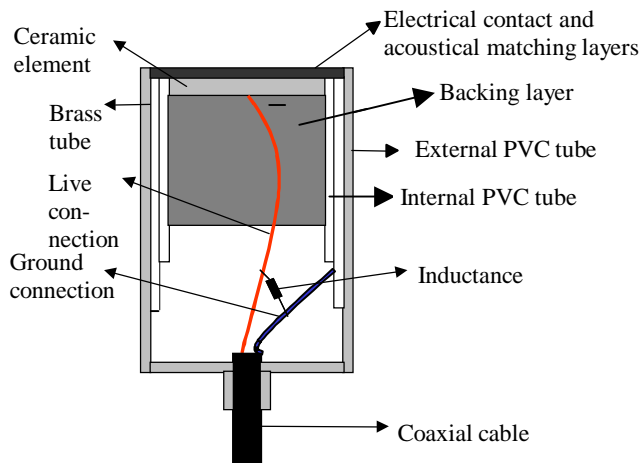


Figure 1. Schematic diagram showing the components of a single element ultrasound transducer.

We have constructed ultrasound transducers with PZT-5A ceramic discs with 12mm diameter and 1mm thickness. We have utilized three different backing layer composition, two acoustical matching layer thickness, and we have also tested the influence of the electrical matching (parallel inductance) in the electromechanical coupling factor.

2.1.1. Backing layer

The backing layer is used to give mechanical support to the transducer, to provide maximal efficiency in the electromechanical coupling, and to prevent reverberation. We constructed transducers with backing layers of different compositions of epoxy with alumina powder and/or Tungsten powder.

Transducers #6, #16 and #19 were constructed with an epoxy and alumina powder backing layer; transducers #5, #8 and #10 with epoxy and Tungsten powder; and transducers #2, #14 and #15 with epoxy, alumina and Tungsten powder. The impedances of the transducers backing layers, showed in Table I, were calculated according to the acoustical impedance of the components used. The acoustical impedance of the PZT-5A is 33.7MRayls.

Table I. Acoustical impedance of the backing layer of each transducer

Backing layer of epoxy and alumina	Z_0 ($10^6 \text{kg/m}^2\text{s}$ or MRayls)	Backing layer of epoxy, alumina and Tungsten	Z_0 ($10^6 \text{kg/m}^2\text{s}$ or MRayls)	Backing layer of epoxy and Tungsten	Z_0 ($10^6 \text{kg/m}^2\text{s}$ or MRayls)
Transducer #6	5.55	Transducer #2	14.4	Transducer #5	14.5
Transducer #16	5.58	Transducer #14	14.2	Transducer #8	16.8
Transducer #19	5.58	Transducer #15	14.2	Transducer #10	16.3

Obs.: All the tables presented in this text, shows the results from the transducers constructed with $3\lambda/4$ acoustic matching layer thickness in gray rows or columns.

2.1.2. Acoustical matching layer

The acoustical matching layer is used to increase the efficiency in the acoustic energy coupling from the transducer to the transmission medium. Commonly it is made with a material that has an acoustic impedance of intermediate value among the impedances of the ceramic (PZT-5A, 33.7MRayls) and the transmission medium (1.6MRayls for biological tissue).

We have used epoxy layers of $\lambda/4$ or $3\lambda/4$ thickness in transducers construction. Matching layers with thicknesses equal to odd multiples of $\lambda/4$ allows acoustic waves that are in phase to be added, and those that are out of phase to be cancelled. The wave length, λ , is calculated by the Equation 2:

$$\lambda = \frac{c}{f_r} \quad (2)$$

Where: c is the propagation speed in the transmission medium (1540m/s for water); and f_r is the resonance frequency

Transducers #2, #5 and #6 were built with $3\lambda/4$ matching layer thickness. The other have $\lambda/4$ matching layer thickness.

2.1.3. Electrical matching.

It is used to match the electrical impedance of the transducer to the electrical impedance of the instrument that works as transmitter (of the electrical signal that drives the transducer) and/or receiver (of the acoustical signal changed into electrical signal by the transducer). We have used the parallel electrical matching, that places an inductor in parallel to the transducer to cancel its intrinsic capacitance (C_0), in the resonance frequency of the thickness mode. The parallel inductance (L_0) can be calculated by Equation 3 [2].

$$L_0 = \frac{1}{(2\pi f_r)^2 C_0} \quad (3)$$

Where: C_0 is the intrinsic capacitance, measured in a frequency below the resonance; and f_r is the resonance frequency.

2.2. Characterization of the ultrasound transducers

After the construction of the ultrasound transducers, with different backing layers compositions and matching layers thicknesses, they were tested to verify if these construction details could be related to the performance parameters. To do the characterization of these transducers, some of the most significant parameters of transducers performance, defined on standards, were chosen to be measured. The following parameters were measured: bandwidth, aperture size, transverse and on-axis profile, and beam spread.

The measurements were made according to international standards [1] [3] [4] [5].

Pulse/echo and transmitter/receiver measurements were made in a water tank. In the transmitter/receiver mode, the transducer under test was the transmitter of ultrasound pulses, and a PVDF (1.0 mm diameter and 20MHz Bandwidth) hydrophone was used as the pulses receiver. Figure 2 shows a schematic diagram of the Acoustical Field Mapping System of the Ultrasound Laboratory (LUS - DEB/FEEC and CEB, UNICAMP).

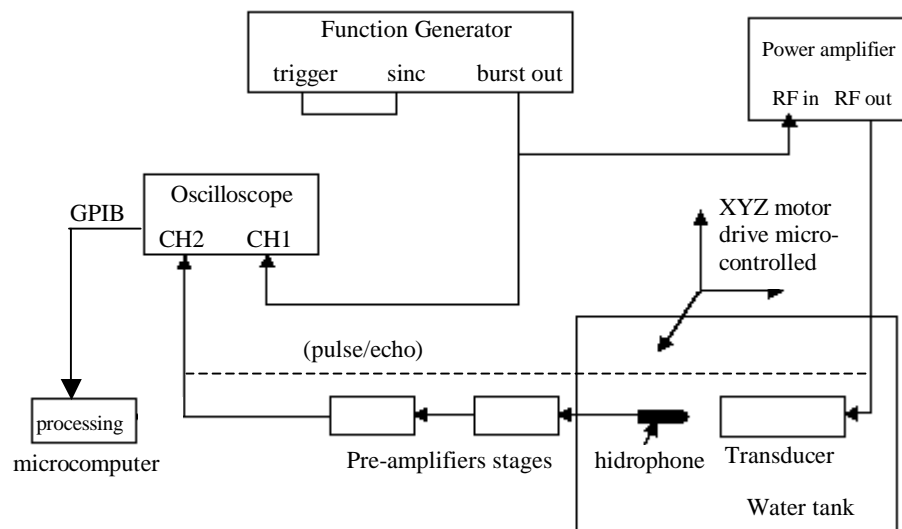


Figure 2. Schematic diagram showing the main components of the Acoustical field Mapping System utilized to do the ultrasound transducers characterization measurements.

The Acoustical field Mapping System consists of a microcomputer controlled XYZ axes displacement unit. In the transmission/reception method, the ultrasound transducer to be mapped is placed in a fixed support, and a punctual PVDF hydrophone is displaced, using step motors, to scan the acoustical field produced by the transducer under test, in transversal or parallel planes to its face. A function generator and a power amplifier are used to apply the electrical signal in the transducer. The ultrasound pulse received by the hydrophone is pre-amplified, digitalized in a scope and sent to the microcomputer to be processed.

In the pulse/echo measurements, some changes in the equipments arrangement are necessary: a flat target is positioned in the far field region of the transducer, and the same transducer acts as the transmitter or the receiver of ultrasonic waves (dashed line in Figure 2).

During the tests, the transducers were excited by a single negative rectangular (-66V) or sinusoidal pulse (66Vpp), in the transducers central frequency (2MHz), repeated at 100Hz.

2.2.1. Bandwidth

According to the international Standard ASTM E-1065 [1] the bandwidth of an ultrasound transducer was determined for the echo of the acoustic pulse generated by a plane reflector put 50mm away from the transducer face. The transducer was excited with a rectangular negative pulse with amplitude of 66V and duration of 240ns. The frequency spectrum of the echo was determined through calculating the echo Fast Fourier Transform (FFT), and the bandwidth was then defined by the difference of the frequencies at which the spectrum intensity decays to 50% of its maximum value: f_{upper} and f_{lower} , according to Equation 4.

$$BW = \frac{f_u - f_l}{f_c} * 100 \quad (4)$$

Where: f_c = transducer central frequency

2.2.2. Transverse profile

To obtain the transverse profile of an ultrasound transducer, we have mapped square areas (30mm x 30mm) parallel to the transducer face, centered in the axial line, along several distances over the axial line, at the near and far fields. The transducer was excited by a single sinusoidal pulse (66Vpp, central frequency of each transducer), repeated at 100Hz.

2.2.3. Aperture size

To measure the aperture size of an ultrasound transducer, first we have obtained the transverse profile of the acoustical field, mapping a plane parallel to the transducers face, at 1.5mm distant from the face of the transducer (near field). Then we have measured the diameter of the -3dB intensity contour plot of the mapping. The diameter value is the aperture size of the transducer.

2.2.4. Axial profile

The axial profile can be measured mapping the field intensity over the axial line from the center of the transducer face to a certain distance. Another way to obtain the axial profile is to map the acoustical field over an area transversal to and centered in the transducer face (ASTM E-1065). This acoustical mapping can be represented in 2D or 3D projections. Finally, the axial profile is the lateral view of the 3D representation of this mapping. Through the 2D acoustical field representation we can determine the intensity field contour plots of -3dB, -6dB and -20dB relative to the maximum field intensity measured.

2.2.5. Beam spread

The beam spread (2ψ) of an ultrasound transducer can be calculated by Equation 5 (ASTM E-1065).

$$2\psi = 2 \arctan W (Z_c - Z_a) \quad (5)$$

Where: Z_a is a distance larger than the transition of near to far field;
 Z_c a distance larger than Z_a ; and
 W is the difference of the width of the ultrasound field (for example, the -3dB intensity contour plot), measured at the distances Z_c and Z_a

3. RESULTS

3.1. Construction of the transducers

Table II shows, for nine transducers constructed, the values of the resonance and anti-resonance frequencies and the effective electromechanical coupling coefficients (with and without the electrical matching) of the

thickness mode (k_t). Coupling coefficients increased after electrical matching of the transducers (except #14), but k_t values were quite different (0.47 to 0.68), and could not be related to any aspect of construction.

Table II also shows values of intrinsic capacitances, measured in a frequency below the resonance frequency, and used to calculate (Equation 3) the parallel inductances used in the electrical matching of the transducers.

3.2. Characterization of the transducers

3.2.1. Bandwidth (BW)

The resultant values of the transducers bandwidth are presented in Table III, and we can observe that:

- values of bandwidth increased after the electrical matching of the transducers;
- transducer #14 showed the largest bandwidth, and it was built with backing layer of epoxy, alumina and Tungsten and with a $\lambda/4$ thickness matching; and
- transducers constructed with $\lambda/4$ thickness matching layer and backing layer composition of epoxy and Tungsten (#8, #10), and epoxy, Tungsten and alumina (#14, #15) showed larger bandwidth than the transducers constructed with the same backing layer composition, but with $\lambda/4$ thickness acoustical matching layer.

Table II. Values of the resonance frequency of the thickness mode, intrinsic capacitances measured in a frequency below the resonance, parallel inductors used in the electrical matching of the transducers, and electromechanical coupling coefficients of the thickness mode, measured before and after the electrical matching of the transducers.

Transducer	f_r (kHz)	f_{ar} (kHz)	C_0 (nF)	L_0 (μ H)	k_t (without L_0)	k_t
#2	2081	2368	1.3	4.5	0.48	0.68
#5	2029	2273	2.2	2.8	0.635	0.64
#6	2051	2352	1.3	4.4	0.49	0.57
#8	2186	2484	5.7	0.93	0.48	0.58
#10	2059	2359	1.8	3.3	0.49	0.60
#14	2192	2540	1.6	3.3	0.51	0.47
#15	2032	2363	1.8	3.4	0.51	0.56
#16	2020	2326	1.9	3.2	0.49	0.60
#19	2180	2449	4.6	1.2	0.47	0.67

Transducers #6, #16 and #19 were constructed with backing layer of epoxy and alumina powder

Transducers #5, #8 and #10 were constructed with backing layer of epoxy and Tungsten powder

Transducers #2, #14 and #15 were constructed with backing layer of epoxy, Tungsten powder and alumina powder.

Transducers #2, #5 and #6 were constructed with $3\lambda/4$ matching layer thickness. The other transducers have $\lambda/4$ matching layer thicknesses.

3.2.2. Transverse profile of the acoustical field

Figure 3 presents the transverse profiles of one of the constructed transducers, measured at two distances (Z_n and $2Z_n$) from the transducers face.

We observed, for all the transducers, that:

- the maximum field intensity was obtained at the distance of the near to far field (Z_n) separation (Table IV);

- the maximum field intensities presented quite varied values for all transducers constructed (Table V), what did not allow to relate this characteristic to the construction details (matching and backing layers);
- transducer #19 showed the largest value of maximum field intensity: 1.46V, and it was constructed with epoxy and alumina backing layer and $\lambda/4$ matching layer thickness.

Table III. Bandwidth of the transducers before and after electrical matching

Epoxy and alumina				
Transducer	BW%	BW % (with L_0)	F_{peak} (MHz)	F_{central} (MHz)
#16	23	29.54	2.05	2.02
#19	16.6	18.76	2.16	2.13
#6	21.2	26.13	2.11	2.06
Epoxy, alumina and Tungsten				
Transducer	BW%	BW %	F_{peak} (MHz)	F_{central} (MHz)
#14	33.49	34.45	2.23	2.18
#15	21.98	26.95	1.98	2.07
#2	15.74	18.35	2.09	2.08
Epoxy and Tungsten				
Transducer	BW%	BW %	F_{peak} (MHz)	F_{central} (MHz)
#8	23.74	25.97	2.18	2.14
#10	21.9	23.39	2.10	2.00
#5	15.75	19.03	2.13	2.10

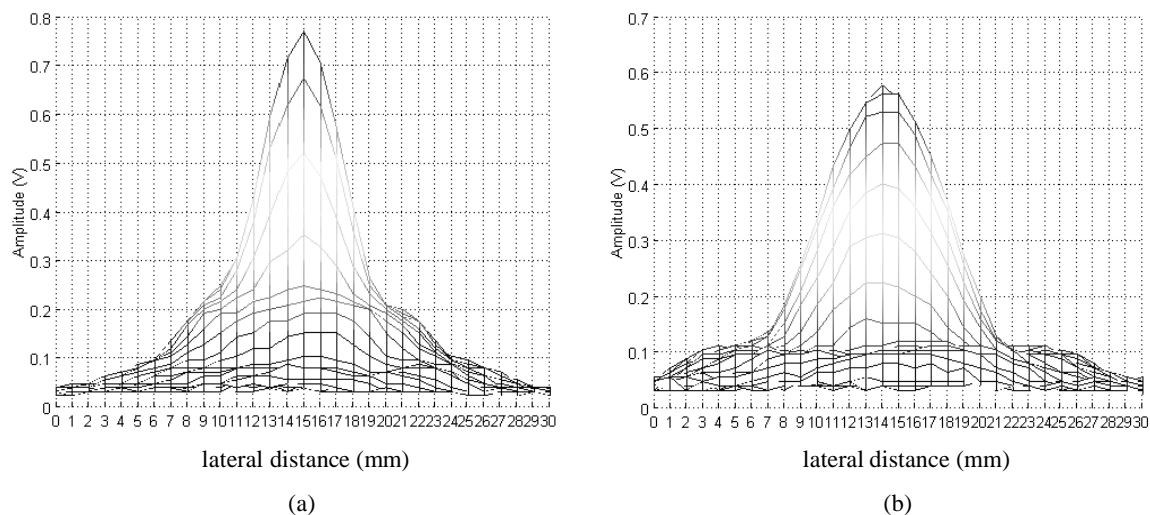


Figure 3. Transverse profiles of the acoustical field produced by the transducer #6, constructed with a backing layer of epoxy and alumina, measured in two distances Z_n (a) and $2 Z_n$ (b).

3.2.3. Aperture size

Figure 4 shows an example of transversal mapping of acoustical field for aperture size determination, and Table IV shows values of aperture size measured for transducers.

Aperture size values, measured for constructed transducers, were between 8.45mm and 9.45mm; this small variation was independent of the composition of the backing layer and thickness of the matching layer.

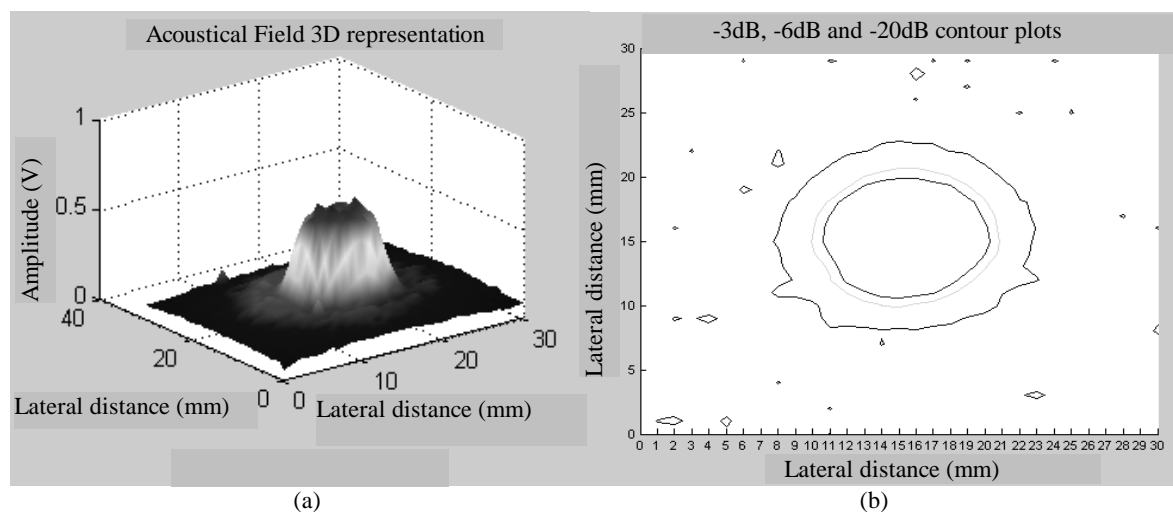


Figure 4. (a) 3D representation of the transversal profile (30mm x 30mm) of the acoustical field produced by transducer #8 and (b) its 2D representation showing the -3dB (inner), -6dB and -20dB (outer) intensity contour plots. The -3dB contour plot diameter is the aperture size of the field.

Table IV. Values of Z_n , Depth and Width of field and Aperture size

Transducer	Aperture size (mm)
Epoxy and alumina	
#16	8.65
#19	9.10
#6	9.45
Epoxy, alumina and Tungsten	
#14	8.90
#15	8.85
#2	9.10
Epoxy and Tungsten	
#8	9.00
#10	8.95
#5	8.45

3.2.4. Axial profile of the acoustical field

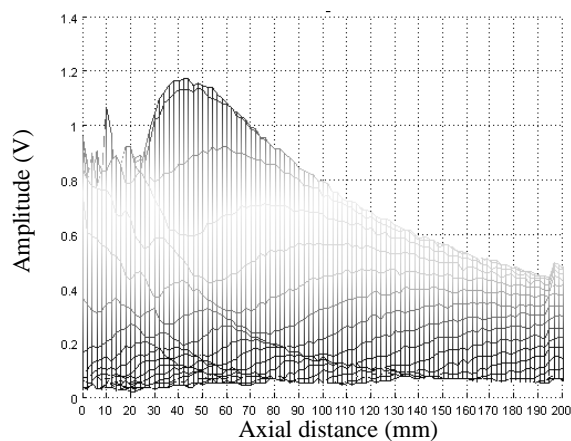
Examples of the axial or on-axis profile of the acoustical field generated by the constructed transducers (one of each backing layer composition group), are shown in Figure 5. From the on-axis profile we determined the depth of field (depth of the -3dB intensity contour plot), width of field (width of the -3dB intensity contour plot), distance of near field to far field transition, and the maximum field intensity.

Table V shows the results obtained from the axial profiles of the acoustical fields produced by the transducers constructed. We can observe that the transducers have similar near field lengths (Z_n) due to that central frequencies values are very close (as shown in Table III).

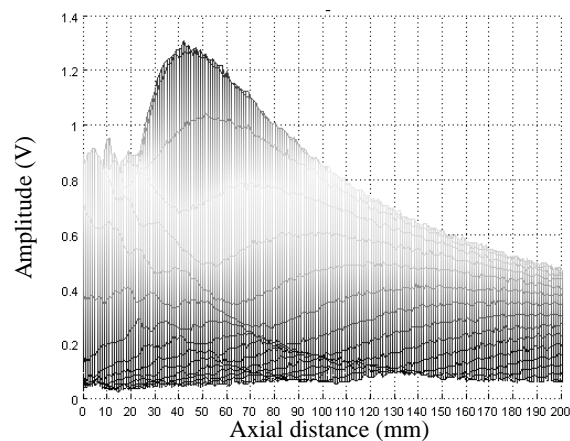
Transducers showed no significant differences among width of field values, but quite varied field intensities and also depth of field, independently of backing layer composition and matching layer thickness.

Table V. Values of Z_n , Depth of field and Width of field

Transducer	Z_n (mm)	Depth of field (mm)	Width of field (mm)	Maximum field intensity (V)
Epoxy and alumina				
#16	47	88	3.5	0.76
#19	51	94	4.0	1.46
#6	48	90	3.9	1.30
Epoxy, alumina and Tungsten				
#14	51	93	3.8	1.25
#15	47	84	4.2	0.73
#2	49	90	4.0	1.21
Epoxy and Tungsten				
#8	51	102	3.8	1.4
#10	48	98	4.1	1.01
#5	47	76	3.2	1.22



(a)



(b)

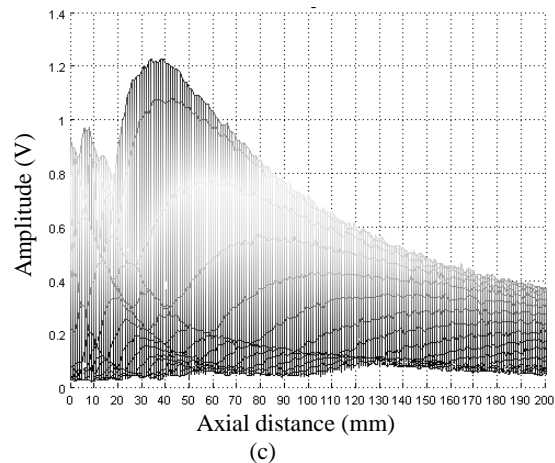


Figure 5. On-axis profiles (lateral views of the 3D representations of the fields mapping on a transversal plane to their faces) of transducers #6 (a), #2 (b) and #5 (c).

3.2.5. Beam spread

Beam spread was calculated for each one of the transducers constructed utilizing Equation 4; these results presented in Table VI, show that:

- the transducers constructed with epoxy and Tungsten backing layer showed smaller beam spread values;
- transducers constructed with $3\lambda/4$ matching layer thickness showed smaller beam spread than transducers with the same backing composition, but with $\lambda/4$ matching layer (except those constructed with epoxy and alumina powder backing layer).

Table VI. Parameters for the Beam Spread (2ψ) calculation, and the maximum relative on-axis field intensity (measured at Z_n) for each transducer

Transducer	Relative Intensity (V) at Z_n	$Z_c = 4Z_n$ (mm)	$Z_a = Z_n$ (mm)	W(mm)	$2\psi (10^{-3})$
#16	0.76	188	47	1.54	21.7
#19	1.46	204	51	1.50	19.6
#6	1.30	192	48	1.43	19.9
Transducer		$Z_c = 4Z_n$ (mm)	$Z_a = Z_n$ (mm)	W(mm)	$2\psi (10^{-3})$
#14	0.73	204	51	1.40	18.2
#15	1.21	188	47	1.60	22.4
#2	1.22	196	49	1.30	17.7
Transducer		$Z_c = 4Z_n$ (mm)	$Z_a = Z_n$ (mm)	W(mm)	$2\psi (10^{-3})$
#8	1.40	204	51	1.20	15.6
#10	1.01	192	48	0.80	11.0
#5	1.22	188	47	0.28	3.9

4. CONCLUSION

Appropriate construction of an ultrasound transducer is decisive for its performance; it allows the available acoustical energy to be transmitted from the transducer face to the next medium, in an efficient way, with reduced losses, instead of being reflected and absorbed by the backing layer, or being attenuated in the front layer. We have constructed transducers with 2 acoustical matching layer thicknesses ($\lambda/4$ and $3\lambda/4$) and 3 backing layer compositions (epoxy and alumina powder, epoxy and tungsten powder, and epoxy and alumina and tungsten powders). Two parameters were evaluated before and after electrical matching of transducers: electromechanical coupling coefficient of the thickness mode of vibration and bandwidth.

Electrical matching layer was responsible for increasing the electromechanical coupling coefficient (k_t) and the bandwidth of the transducers. Results also showed that $\lambda/4$ and $3\lambda/4$ acoustical matching layer thicknesses limit the transducers bandwidth. Transducers constructed with $\lambda/4$ matching layer thickness, compared to the transducers with $3\lambda/4$ thickness, presented larger bandwidth, except for the transducers with backing layer composed of epoxy and alumina powder. Transducers which backing layers were composed of epoxy and Tungsten powder, presented smaller beam spread values than the other compositions. Some of the parameters evaluated, as aperture size, depth of field and maximum field intensity, could not be related to any of the construction details.

ACKNOWLEDGEMENTS

CAPES, FAPESP, FINEP (RECOPE) are gratefully acknowledged for the financial support.

REFERENCES

1. ASTM E-1065 1999. *Standard Guide for Evaluating Characteristics of Ultrasonic Search Units*, 1999.
2. DESILETS, C. S.; FRASER, J. D.; KINO, G. S. - The Design of Efficient Broad-Band Piezoelectric Transducers. *IEEE Transactions on Sonics and Ultrasonics*, v. su-25, n. 3, p. 115-125, 1978.
3. IEC-1390 - *Ultrasonics Real Time Pulse-Echo Systems: Test Procedures to Determine Performance Specification.*, 1996.
4. IEEE American National Standard Std 790 - *IEEE Guide for Medical Ultrasound Field Parameter Measurements*, 1989.
5. IEEE American National Standard Std 176 - *IEEE Standard on Piezoelectricity*, 1978.
6. INOUE, T.; OHTA, M.; TAKAHASHI, S. - Design of Ultrasonic Transducers with Multiple Acoustic Matching Layers for Medical Applications, *IEEE Transactions on Ultrasonics, Ferroelectrics and Frequency Control*, v. 34, no. 1., 1987.
7. LOCKWOOD, G. R.; TURNBULL, D. H.; FOSTER, F. S. - Fabrication of High Frequency Spherically Shaped Ceramic Transducers, *IEEE Transactions on Ultrasonics, Ferroelectrics and Frequency Control*, v. 41, n. 2., 1994.
8. MITRA, R.; SAKSENA, T. K. - Study on the Vibrational Characteristics of Ultrasonic Transducers Using Tapered Piezoelectric Ceramic Elements, *Journal of the Acoustical Society of America*, v. 58, n.2., 1995.
9. SAYERS, C. M.; TAIT, C. E. - Ultrasonic Properties of Transducer Backing, *Ultrasonics*, v.22, n. 2., 1984.